Sedimentary thickness variations and deformation intensity during basin inversion in the Flinders Ranges, South Australia

MIKE SANDIFORD*, EIKE PAUL and THOMAS FLOTTMANN

Department of Geology and Geophysics, University of Adelaide, South Australia

Abstract—The central and northern parts of the Adelaide fold belt in the Flinders Ranges, South Australia, consist of a sequence of Neo-Proterozoic–Cambrian sediments overlying a Meso-Proterozoic basement complex, both of which were mildly deformed in an intracratonic setting during the ∼500 Ma Delamerian orogeny. The fold belt lies within a prominent heat flow anomaly (average heat flows of ∼90 mWm^{-2}) reflecting extraordinary enrichments in heat producing elements in the Meso-Proterozoic basement, suggesting that anomalous thermal regimes may have been significant in localising Delamerian deformation. However, spatial variations in deformation intensity correlate more closely with variations in the thickness of the sedimentary sequence than with observed variations in heat flow, suggesting that the thickness of the sedimentary blanket plays a crucial role in localising Delamerian deformation during basin inversion. We use simple numerical models of lithospheric strength to investigate the potential role of sedimentary thickness variations on the distribution and style of deformation, focussing on the impact of a variable thickness sediment pile deposited above a 'radioactive' basement. We show that for thermal parameters appropriate to the Flinders Ranges, Moho temperatures may vary by ∼25–30°C for every additional kilometre of sediment. For a 'Brace–Goetze' lithospheric rheology, controlled by a combination of temperature-dependent creep processes and frictional sliding, the observed variations in thickness of the sedimentary pile are sufficient to cause dramatic reductions in the vertically-integrated strength of the lithosphere (by many orders of magnitude), thereby providing a plausible explanation for observed correlation between sediment thickness and deformation intensity during basin inversion. © 1998 Elsevier Science Ltd. All rights reserved

INTRODUCTION

The modern view of orogenic belts as manifestations of relative motion across active plate boundaries implies, at the largest scale, that deformation intensity is related to proximity to plate boundaries. However, it is well known that both ancient and modern orogenic belts show significant regional variations in both style and intensity of deformation that are not readily explicable in terms of proximity to plate boundaries. One of the most spectacular examples of this in the modern Earth is the partitioning of active deformation evident around the Tarim Basin in Central Asia (e.g. Neil and Houseman, 1997). While such regional variations in deformation intensity (and style) are likely to reflect variations in the mechanical response of the orogen, the specific controls that mediate the mechanical response of the continental lithosphere remain poorly understood. This is particularly true of deformations involving basement reactivation in intracratonic settings (e.g. Rogers, 1995).

The Adelaide fold belt in South Australia (Fig. 1) consists of a Neo-Proterozoic to Cambrian sedimentary (cover) succession deformed along with its Meso-Proterozoic basement in the late Cambrian–early Ordovician (∼500–490 Ma) Delamerian Orogeny. Like many fold belts, it shows systematic regional variations in style and intensity of deformation. At the largest

scale, the fold belt can be divided into three distinct zones characterised by different styles and intensities of deformation (Marshak and Flottmann, 1996);

- a southern zone, including the southern Adelaide fold belt (with orogenic shortening of 30–50%) and the Nackarra Arc (where orogenic shortening strains average >6%—see Fig. 1b);
- a central zone (the central Flinders zone), characterised by shortening <5% (Fig. 1b); and
- a northern zone (the northern Flinders zone) characterised by intermediate deformation intensity with shortening averaging ∼11% (Fig. 1b).

Late Cambrian palaeogeographical reconstructions place the active continental margin to the southeast of the preserved fragments of the fold belt (Coney *et al.*, 1990), with the central and northern parts of the fold belt bounded by the older, relatively undeformed cratonic blocks of the Gawler Craton (to the west) and the Curnamona Craton (to the east). In parts of the fold belt, the deformation has involved the basement, which is now exposed as a series of inliers in the north (the Painter and Babbage Inliers), in the east (the Willyama Inliers) and in the south (the Houghton and Myponga Inliers). Elsewhere the deformation has detached the cover sequences from the underlying basement (e.g. the Nackarra Arc).

Paul *et al.* (1998) have shown that the first order variations in the deformation intensity and the extent of basement reactivation in this central and northern
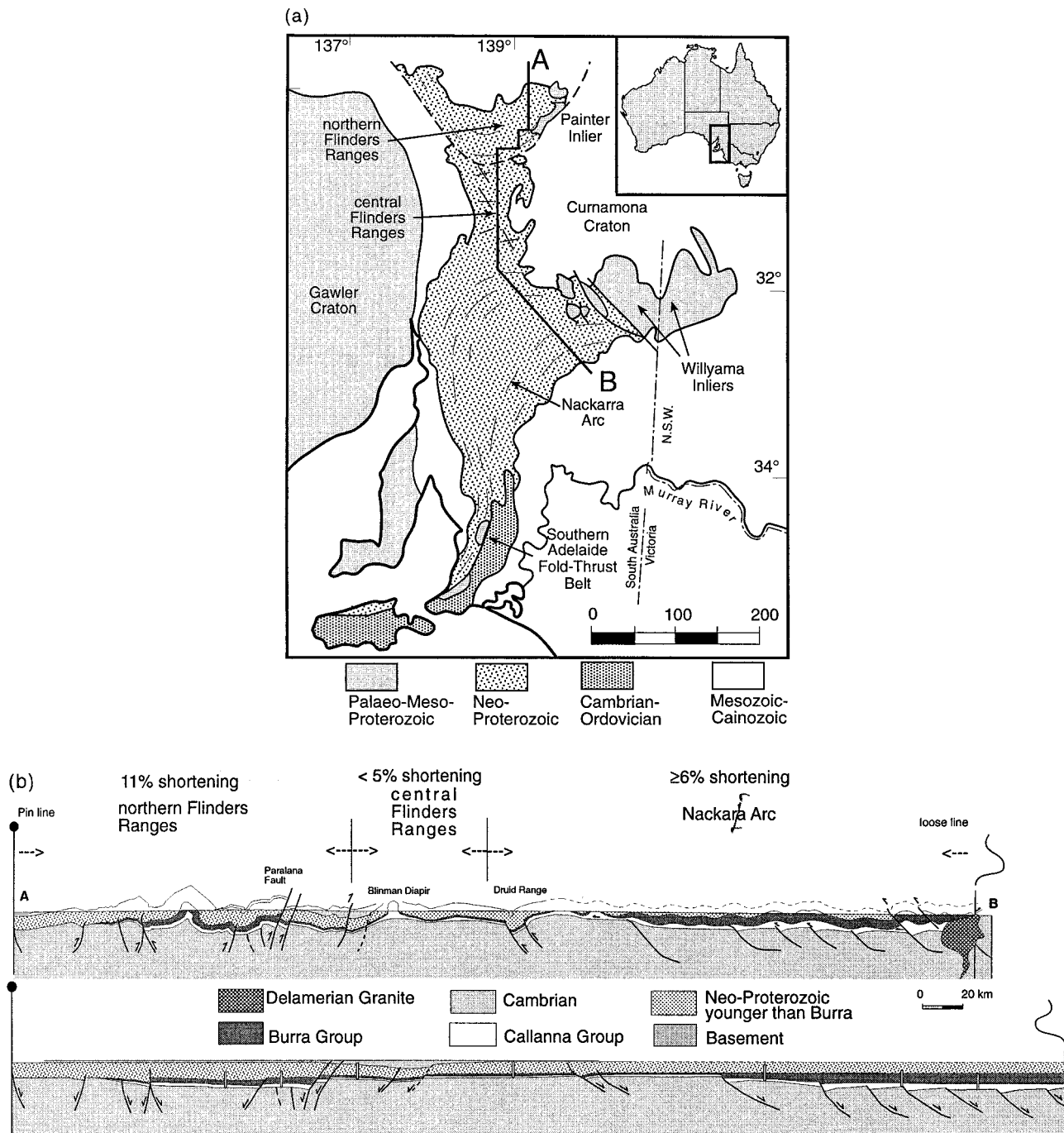
*E-mail:msandifor@geology.adelaide.edu.au

Fig. 1. (a) Location map of the Adelaide Fold belt showing the line of the section shown in (b). (b) Synthetic structural and restored section from the northern Flinders Ranges (A) through the central Flinders Ranges, to the Nackarra Arc (B), based on Paul et al., (1998) and Marshak and Flottmann (1996). The distribution of deformation intensity based on estimates of shortening from these studies show a marked reduction in the region of the central Flinders Ranges, where the sedimentary succession is thinnest (as shown by the vertical scale-bars). The heavily stippled layer is the Burra Group, and is underlain by the Callana Group and overlain by the Umberatana and Wilpena Groups and, finally,

part of the fold belt correlate with spatial variations in stratigraphic thickness (Fig. 2), with much of the shortening strain localised on reactivated growth faults. Together with the demonstrably intracratonic setting for the central and northern parts of the fold belt, this raises a number of important questions, including:

- why is significant Delamerian deformation only found where there is a significant thickness ($\gtrsim 5$ km) of Neo-Proterozoic–Cambrian sediment; and
- what specific controls have localised the (relatively) more intense deformation in the northern parts of the fold belt?
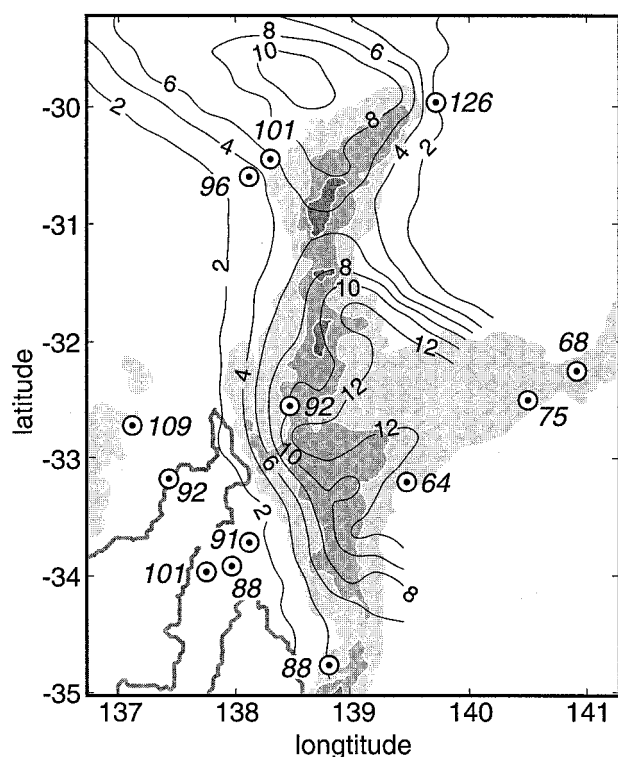
Fig. 2. Generalised isopach map for Neo-Proterozoic sequences in the northern Flinders Ranges–central Flinders Ranges–Nackarra Arc region of the Adelaide fold belt, based on data summarised in Preiss (1987). The isopach contour interval is 2 km. Heat flow measurement locations are indicated by 'bullets', with the measured values in units of mWm^{-2} indicated by the italicised numbers. Topography is indicated by grey-level shading (for each 200 m interval).

The purpose of this paper is to further explore the role stratigraphic thickness plays in mediating the intensity of deformation using quantitative numerical models which couple the thermal and mechanical state of the deforming orogen at the time of onset of deformation. Specifically, we analyse the modern day heat flow regimes to develop constraints on thermo-mechanical models designed to evaluate the parameters controlling the style and distribution of Delamerian deformation in the northern and central Flinders Ranges. We begin with a brief summary of the sediment thickness distribution in the northern and central Flinders Ranges. This is followed by a discussion of thermal regimes during the terminal stages of basin development using constraints from modern heat flow as well as inferences drawn from metamorphic assemblages developed during the Delamerian orogeny.

STRATIGRAPHIC THICKNESS VARIATIONS IN THE CENTRAL AND NORTHERN FLINDERS RANGES

The Adelaide fold belt deforms a thick succession of sediments deposited in a series of rift-sag basins during the Neo-Proterozoic and Cambrian (Preiss, 1987;

Jenkins, 1990; Jenkins and Sandiford, 1992). These deformed and in part metamorphosed sediments are now mostly confined to a region of elevated topography forming the Flinders and Mount Lofty Ranges (Fig. 2); the modern topography reflects the reactivation of the fold belt during the late Tertiary. During the Delamerian Orogeny, the northern and central parts of the Adelaide fold belt were surrounded by cratons (the Gawler Craton, Stuart Shelf and Curnamona Craton), which were covered at most by only thin veneers of Neo-Proterozoic sediment and which remained essentially undeformed (Preiss, 1987). As shown by Paul et al. (1998), the similarity in the patterns of deformation intensity in the fold belt and thickness variations in the sedimentary pile, holds not only at the scale of the fold belt, but also at the intrabasinal scale. In the central and northern Flinders Ranges the Neo-Proterozoic cover succession, collectively known as the Adelaidean, has a cumulative maximum thickness of around 20 km, reflecting spatial and temporal variations in the depocentres through the ~300 Ma depositional history. The maximum thickness in any specific locality is about 14 km in the Nackarra Arc (Fig. 2). In the central Flinders Ranges, in the region immediately north of the Nackarra arc, somewhat condensed successions are preserved with total cumulative thickness of around ~7–8 km (Preiss, 1987). In contrast, the northern Flinders Ranges represent a persistent depocentre, with the sedimentary pile locally as much as 12 km thick. As outlined earlier and shown in the synthetic sections in Fig. 1, previous structural studies by Paul et al. (1998) and Marshak and Flottmann (1996) have shown that the overall deformation intensity varies markedly across the northern and central parts of the fold belt, being greatest in the Nackarra arc (local shortening of ~20%) and the northern Flinders Ranges (local shortening ~10–20%) sectors, and lowest in the central Flinders Ranges (local shortening < 5%) where the sedimentary succession is thinnest.

THERMAL CONSIDERATIONS

The coincident patterns of sediment thickness and deformation intensity during 'basin inversion' suggest the possibility that deformation may have been localised by some process intrinsic to the development of the basin. Two possibilities spring to mind. Firstly, the basin inversion (as well as basin formation) may have been localised by fundamental and long-lived regional variations in lithospheric strength. Alternatively, the development of the basin itself may have altered the mechanical properties of the lithosphere, thereby helping to localise subsequent deformation. In as much as lithospheric strength is generally considered to be temperature sensitive (e.g. Brace and Kohlstedt, 1980; Sonder and England, 1986; England, 1987; Ord and

Hobbs, 1989), we might expect to be able to evaluate the plausibility of these two models with reference to known or inferred constraints on the regional thermal structure at the time of deformation. Because the modern heat flow field contains information about the distribution of heat sources at depth, it can be used to constrain thermal regimes in times past. In this section we use constraints from the modern heat flow field, as well as observations on metamorphic conditions in the deforming pile, as a basis to evaluate these alternative possibilities. We pay particular attention to the relative contributions of mantle (or reduced) heat flow and crustal sources to the modern day heat flow, in order to constrain deep lithospheric thermal regimes attendant with basin development and Delamerian deformation.

The South Australian heat flow field

The present day heat flow records for South Australia and western New South Wales, largely based on the compilation of Cull (1982), are shown in Fig. 3. The available data comprise 23 individual heat flow records and show systematic variations in surface heat flow (q_s) across South Australia. The measured heat flow increases from ~50 mWm^{-2} in the western Gawler Craton to greater than 90 mWm^{-2} in the vicinity of the western boundary of the Adelaide fold belt before falling to ~65–75 mWm^{-2} in the vicinity of the Willyama Inliers (including Broken Hill) in the eastern parts of the fold belt. These data clearly show that the western boundary of the fold belt is located within a province of unusually high heat flow. Geologically, this anomalous heat flow province corresponds with regions in which the major crustal growth occurred in the Palaeo-Proterozoic through Meso-Proterozoic provinces, and is clearly 'hotter' than the older fragments of the western Gawler craton where the major crust

forming events are Archaean in age. This South Australian heat flow anomaly forms part of a broad band of elevated surface heat flow through the central part of Australia termed the 'Central Australian heat flow province' by Sass and Lachenbruch (1978). Importantly, this province corresponds approximately with the distribution of Palaeo- and Meso-Proterozoic crust in the Australian continent including the Mount Isa Inlier ($q_s\sim80$ mWm^{-2}), Tennant Creek ($q_s\sim100$ mWm^{-2}) and the U-rich provinces in the north of the Northern Territory ($q_s\sim100$ mWm^{-2}).

The observation that the heat flow anomaly extends beyond the margins of the fold belt, suggests that it reflects anomalous heat production rates in the basement rocks, an interpretation supported by the widespread U-mineralisation in Meso-Proterozoic rocks in the various cratons surrounding the Adelaide fold belt. The local influence of elevated U-concentrations on the heat flow field has been demonstrated in a detailed study by Houseman *et al.* (1989) around the Roxby Downs Cu–U–Au–Ag deposit on the Stuart Shelf. This is a region of the Gawler craton bordering the Adelaide fold belt covered by a thin veneer of essentially undeformed Neo-Proterozoic sediment. This study revealed significant variation in heat flow on a 10 km scale, with anomalies directly related to U-mineralisation. In this region a background heat flow of around 75 mWm^{-2} is observed at distances of >5 km from the deposit with heat flow rising to 128 mWm^{-2} above the deposit. Since U-mineralisation is believed to predate deposition of the Neo-Proterozoic sediments of the Adelaide Geosyncline and Stuart Shelf (Johnson and Cross, 1995), it seems likely that the basement beneath the Adelaide fold belt inherited similar spatial variations in heat production.

The geology of the Mount Painter region

Dramatic testimony to the role of the radioactive basement in mediating the thermal regime both in the modern environment and during the development of the Delamerian orogen is provided by observations near the Painter and Babbage Inliers in the far northeast of the fold belt where the recorded modern day heat flow is 126 mWm^{-2} (Cull, 1982). Because of the importance of this region in understanding the controls on thermal regimes developed during Delamerian deformation, we provide a brief description below.

In the Mount Painter region Meso-Proterozoic granitic gneisses and metasediments exposed in the Painter and Babbage Inliers form the cores of regional anticlinal culminations (Fig. 4; see Paul *et al.*, 1998). Along the southern part of the Painter Inlier, a more-or-less complete Neo-Proterozoic succession (begining with the Callana Group sediments) rests unconformably upon the basement (Fig. 1b). Around the Babbage Inlier and the northern part of the Painter Inlier, the oldest Neo-Proterozoic units are missing
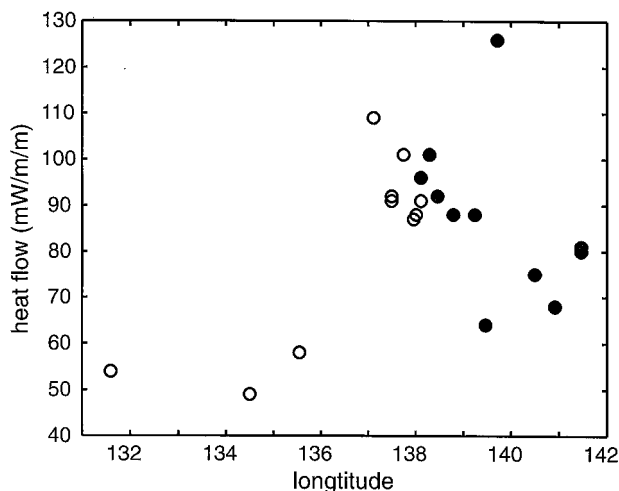

Fig. 3. Heat flow data plotted as a function of longitude indicate a broad anomaly centred on, but significantly wider than, the distribution of modern Flinders Ranges, which almost exactly coincides with the Adelaide fold belt.
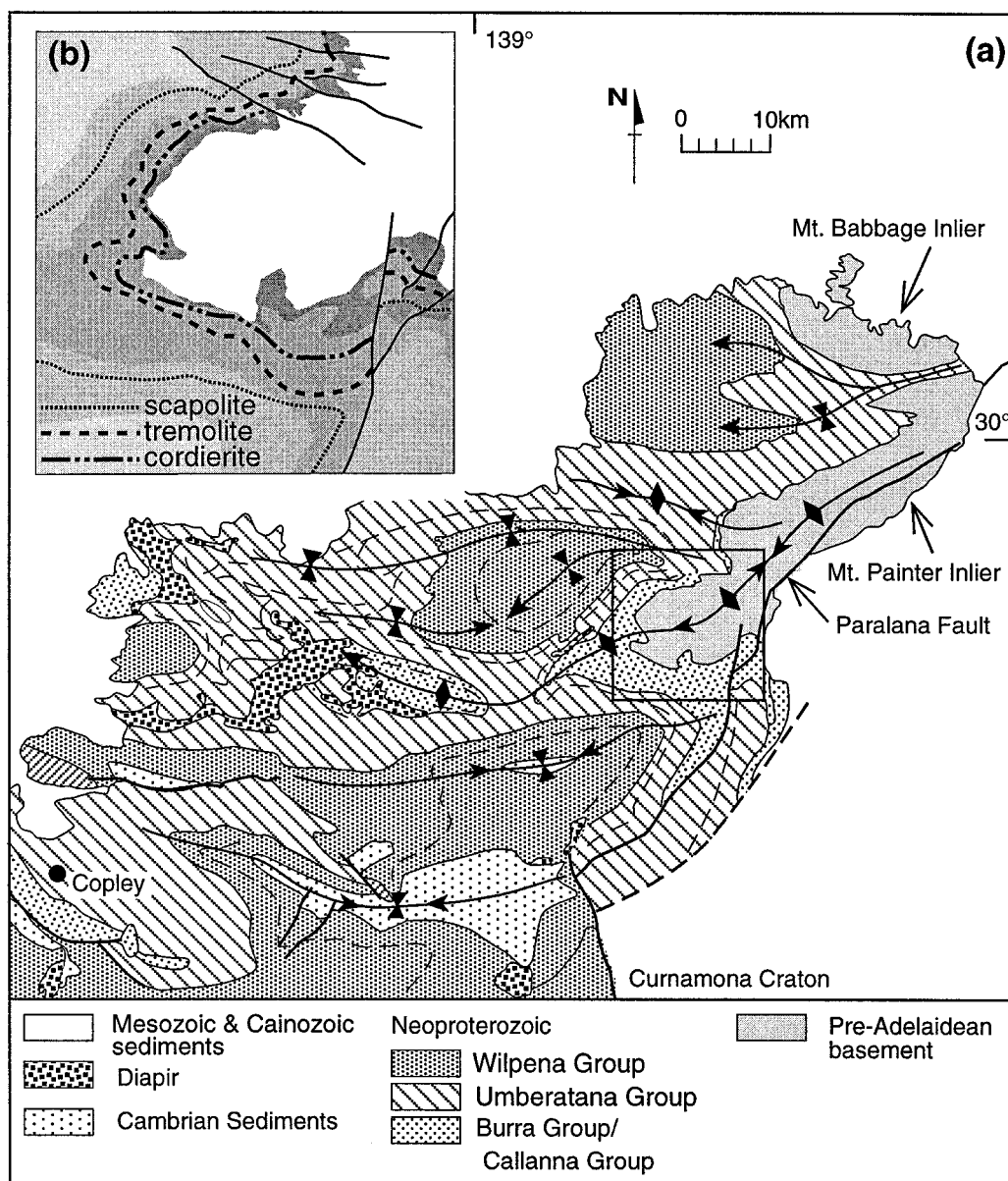
Fig. 4. (a) Geology of the Mount Painter region in the northern Flinders Ranges, showing the Arkaroola anticline as a large-amplitude, west-plunging, basement-cored fold. (b) Detail of nose of anticline showing folding of a regional isograd structure that is essentially concordant with the basement–cover unconformity (see Mildren and Sandiford, 1995).

(the Callana and Burra Groups) with Umberatana Group glacials resting unconformably on the basement. The anticlinal structures exposing the basement form part of a regional E–W trending fold train extending some ~100 km across the northern Flinders Ranges. Basement is only exposed along the eastern part of this fold train, where fold axes swing to a northeast trend as they merge with the Paralana fault system. This fault represents a major structural discontinuity in the region separating the Adelaide fold belt in the west from the Curnamona Craton to the east. Syn-sedimentary movement along this system is indicated in changing facies distributions in Callana and Burra Group sediments, while post-Delamerian movement is evident by thrusting of the Painter Block

above Mesozoic and Cenozoic sediments that presently cover the Curnamona Craton. This post-Delamerian ramping along the Paralana Fault has resulted in the Delamerian structures now being exposed in oblique profile. In the Mount Painter region, the folds are tight, with interlimb angles of around 40°, wavelengths of around 40 km and amplitudes of ~10 km implying strong coupling of basement and cover sequences during deformation (see Paul et al., 1998).

One of the most striking (and unusual) features in the Painter region is the metamorphic character of the Neo-Proterozoic cover sequences surrounding the inliers. Here, the cover sequence shows rapid changes in metamorphic grade approaching the basement–cover unconformity, with essentially unmetamorphosed

(or very low metamorphic grade) sequences at distances of around 5 km grading into lower amphibolite facies at the unconformity. Progressive metamorphism is indicated by the development of tremolite-in, and cordierite-in isograds in the Burra and Callana Groups, with isograds essentially concordant with the basement cover unconformity (as shown in the inset in Fig. 4). The occurrence of diopside- and cordierite-bearing assemblages in the cover sequences immediately above the unconformity implies temperatures in excess of 500°C. While only poorly constrained by quantitative barometry, estimates of the pressures of these metamorphic rocks of approximately 3 kbars are compatible with reconstructed thickness of the local sedimentary pile (10–11 km, Paul et al., 1998), suggesting average thermal gradients in the upper crust of 50°C km^{-1}. The unusual metamorphism in this region can be directly attributed to the extraordinarily high concentrations of the heat producing elements in the exposed basement (Sandiford et al., 1998). For example, the granitic rocks comprising ~60% of the basement exposures typically have heat production rates in the range 8–20 μWm^{-3}, and locally as high as 40 μWm^{-3}. Sandiford et al. (1998) have estimated an area-averaged heat production of 9.9 μWm^{-3} for the Painter and Babbage Inliers at the time of the Delamerian Orogeny and shown that such exceptionally high heat production rates can account for the modern day heat flow.

Origins of the South Australian heat flow anomaly

The observations outlined above indicate that the Adelaide fold belt is confined within a zone of anomalous heat flow associated with unusual enrichments in heat producing elements in the Meso-Proterozoic basement sequences. One way of characterising the enrichment is to estimate the contribution of crustal heat sources to the observed surface heat flow. In order to do this, the crustal contribution (q_c) to the surface heat flow must be distinguished from the mantle or reduced heat flow (q_r). The traditional procedure for this involves regressing the observed heat flow data against surface heat production data (Lachenbruch, 1968). On a global scale such regression typically yields estimates for mantle heat flows in the range 20–40 mWm^{-2} with crustal contributions in Proterozoic terranes contributing some 20–40 mWm^{-2}. Sass and Lachenbruch (1975) showed that a regression of the available heat flow–heat production data for South Australian basement rocks yields an estimate for the reduced heat flow of ~30 mWm^{-2}, implying that the remainder of the observed surface heat flow (~45–60 mWm^{-2}) is contributed by crustal heat sources (U, Th, K). However, two important additional lines of evidence suggest that the reduced heat flow must be somewhat lower than 30 mWm^{-2}.

Firstly, as shown by Jaupart (1983), in regions where the heat production parameters show significant lateral variations (such as the Proterozoic of Australia, Houseman et al., 1989) the effect of lateral conduction of heat between different heat flow provinces may have a considerable effect on the heat production–heat flow relationship. This effect always results in the regression technique overestimating the reduced heat flow (as well as underestimating the characteristic length-scale for heat production in the crust), with the magnitude of the error dependent on the horizontal length-scale for heat production variation. For lateral variations of the type documented by Houseman et al. (1989) from the Roxby Downs region, this 'Jaupart'-effect can be severe with the regression technique overestimating reduced heat flows by as much as 100%. The second line of evidence supporting elevated crustal sources rather than reduced heat flow as a prime contributor to the central Australian heat flow province relates to estimates of the modern lithospheric thickness in this South Australian heat flow province. Assuming that most lithospheric heat sources are contained within the crust, then the reduced heat flow is a proxy for the thickness of the mantle lithosphere, with q_r reducing with increasing mantle lithospheric thickness:

$$q_r = kT_{ml}/z_{ml}$$

where T_{ml} is the temperature difference across the mantle lithosphere, z_{ml} is the thickness of the mantle lithosphere and k is the thermal conductivity of the mantle lithosphere. Independent estimates of the lithospheric thickness can therefore be used to estimate the mantle heat flow. Recent seismic tomographic studies by Zeilhaus and van der Hilst (1996) show anomalous velocities to depths of at least 200 km (and possibly 250 km) beneath the central Australian Proterozoic terranes. Associating such velocity anomalies with lithospheric mantle implies a lithospheric mantle thickness in excess of 150 km, and for thermal conductivities of 3 Wm^{-1} K^{-1}, and Moho temperatures of around 300–700°C, implies q_r is in the range 10–15 mWm^{-2}. These estimates of q_r imply that crustal heat sources contribute the bulk of the observed heat flow in South Australia, contributing ~75 mWm^{-2} to the observed heat flow in the Flinders Ranges and ~60 mWm^{-2} to the background heat flow observed in the Houseman et al. (1989) Roxby Downs study.

Significance of the heat flow data

The data presented in the previous section support the notion that the anomalous heat flow in the vicinity of the Adelaide fold belt is associated with the unusually high levels of heat production in the Proterozoic basement. However, the data also show that the heat production heat flow anomaly is significantly broader than the distribution of Delamerian strain, which more

closely mimics the isopach thickness of the Neo-Proterozoic sedimentary cover. We believe this interpretation implies a fundamental role for the sedimentary blanket thickness in localising deformation. In the following section we explore the thermal and mechanical plausibility of this scenario using default thermal parameters appropriate to the modern day heat flow regime in the Flinders Ranges (i.e. $q_c = 70$ mWm^{-2} with heat production concentrated in the upper parts of the basement sequence).

THERMAL CONTROLS ON STRENGTH DISTRIBUTION IN THE CONTINENTAL CRUST

An important outcome of our earlier discussion is the insight that the development of the sedimentary pile prior to the Delamerian Orogen resulted in significant but variable burial of a radioactive basement. The thermal parameters relevant to this hot basement are reflected in the modern heat flow field and in the measured heat production rates of exposed basement rocks in and around the fold belt. These parameters can be used to reconstruct plausible thermal regimes attendant with basin development at the time of onset of the Delamerian orogeny. In this section we explore the thermal and mechanical consequences of burying such a 'hot' basement sequence. Because the last significant rifting event to precede basin inversion occurred at around 630 Ma (Jenkins, 1990), we can assume that the lithosphere was close to thermal equilibrium by the time of Delamerian deformation at ~500–490 Ma.

We are concerned here with the first-order thermal response of the lithosphere to the burial of hot basement beneath a sedimentary cover. At the lithospheric scale this response is not sensitive to the small-scale variations in heat production and thermal conductivity associated with individual map-scale geological units, as such variations are dampened relative to the longer wavelength variations. Consequently, it is sufficient to prescribe the heat production and thermal conductivity variation in a very general form. In this analysis we are concerned mainly with variations in the depth distribution of heat production associated with progressive burial and we have therefore ignored the role of vertical thermal conductivity variations and horizontal variations in heat production. It is worth noting, however, that the thermal conductivity of sedimentary blanket is likely to be less than that of the granitic basement. In the context of the discussion below, the effect of such an insulating blanket will be to further enhance any thermal effects introduced by burial of an anomalously 'hot' basement.

Because the variations in heat production at the small scale are irrelevant to the first-order thermal response of the lithosphere, we adopt a simple distribution of heat production to model the consequences

of burying a 'hot' basement which is characterised by a heat production maxima at a discrete level within the crust (Fig. 5a). The distribution we use is:

$$H(z) = H_i \exp\left(\frac{-(z - z_i)^2}{h_r^2}\right). \qquad (1)$$

In this distribution the maximum heat production occurs at depth z_i. The parameter h_r is used in its familiar sense of prescribing the length-scale of heat production variation (in this case it provides a measure of the spread of the heat production within the hot layer, with the heat production falling to H_i e^{-1} at depths $z_i \pm h_r$).

In the steady state, the integrated crustal heat production (q_c) represents the crustal contribution to the surface heat flow

$$q_c = \int_0^{z_c} H(z)\, dz.$$

For the heat production distribution given by equation (1), the integrated crustal heat production is given by

$$q_c = \frac{H_i h_r \sqrt{\pi}}{2}\left(\text{Erf}\left(\frac{z_c - z_i}{h_r}\right) + \text{Erf}\left(\frac{z_i}{h_r}\right)\right). \qquad (2)$$

The thermal effects of such a heat production distribution are readily obtained once we prescribe the boundary condition that defines the base of the lithosphere. There are two models for this basal boundary
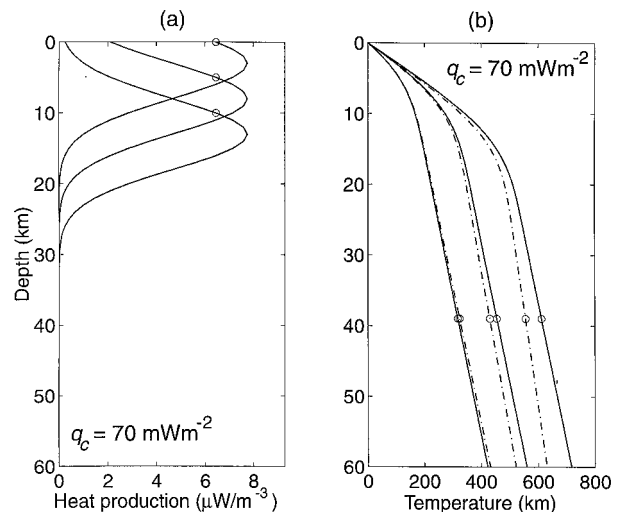

Fig. 5. Illustration of heat source distributions (a), and calculated geotherms (b), based on our model for the burial of radioactive basement beneath a less radioactive sequence, as discussed in the text. The figures show explicitly burial depths of the basement–cover interface at 0, 5 and 10 km. In (b), the solid lines correspond to solutions of equation (3) appropriate to a thermally stabilised lithosphere, while the dotted lines show the equivalent solution for a compositionally stabilised lithosphere. We have used a thermal parameter range based on our analysis of the modern surface heat flow field which shows a broad anomaly averaging ~90 mWm^{-2}. Explicitly, the parameters used are $H_i = 7.75$ μWm^{-3}, $q_c = 70$ mWm^{-2}, $q_m = 20$ mWm^{-2} ($z_1 = 225$ km), $k = 3.0$ Wm^{-1} k^{-1}.

condition, both of which are equally plausible, but which yield significant differences in the thermal structure of the deeper crust. The most commonly used model is that of a thermally stabilised lithosphere (TSL) in which the lower boundary condition is one of constant heat flux (geologically this corresponds to the model of a thermal plate in which the convective processes in the deeper mantle provide a constant heat flow at the base of the plates). The steady-state temperature distribution in the lithosphere of thickness z_c subject to a basal heat flux q_m with a depth-independent thermal conductivity k is:

$$T(z) = -\frac{q_m z}{k} + \frac{H_i h_r^2}{2k}\left(\exp\left(-\frac{z_i^2}{h_r^2}\right) - \exp\left(-\frac{(z_i - z)^2}{h_r^2}\right)\right)$$

$$+ \frac{h_r H_i \sqrt{\pi}}{2k}\left(z\,\mathrm{Erf}\left(\frac{z_c - z_i}{h_r}\right) + (z_i - z)\,\mathrm{Erf}\left(\frac{z - z_i}{h_r}\right)\right.$$

$$\left. + z_i\,\mathrm{Erf}\left(\frac{z_i}{h_r}\right)\right). \tag{3}$$

An alternative geothermal model is that of a compositionally stabilised lithosphere (CSL), in which the lower boundary condition is given by a constant temperature at specified depth.

A range of solutions for both the thermally- and compositionally-stabilised lithospheric models are shown in Fig. 5(b). The illustrated solutions differ only in the depth of burial of the heat producing layer, and therefore simulate the effects of burying a radiogenic basement sequence beneath a sedimentary cover (Fig. 5b explicitly shows burial depths corresponding to a sedimentary blanket thickness of 0, 5 and 10 km). The thermal parameters used in constructing Fig. 5(b) are set so that $q_c = 70$ mWm^{-2}, as appropriate to the modern day heat flow regime in the Flinders Ranges. An important feature illustrated by Fig. 5(b) is the sensitivity of the deep crustal temperatures to the depth of the heat production anomaly (or, equivalently, the depth of the basement–cover interface). The definition of the Moho temperature requires understanding of the way Moho depth varies with sediment thickness. In the calculations presented here we assume that Moho depth is approximately constant throughout, as is appropriate to an isostatically balanced crustal section where variations in sediment thickness reflect variations in crustal stretching. Depending on the lower boundary condition (that is, either thermally or compositionally stabilised), the Moho temperature increases by between 24 and 30°C for every additional kilometre of sediment above the basement–cover interface. This point is illustrated more clearly in Fig. 6 which shows how the Moho temperature varies with sedimentary blanket thickness for a range of different crustal thermal parameters ($q_c = 30, 50, 70$ and 90 mWm^{-2}). Figure 6 shows that for more typical values

of q_c ($\sim$30–40 mWm^{-2}) the Moho temperature rises by about 9–22°C per kilometre of additional sediment.

Rheological considerations

Lithospheric rheology is generally regarded to be temperature dependant and particularly sensitive to the thermal state of the upper mantle (e.g. Sonder and England, 1986; England, 1987). A popular, generalised model for lithospheric rheology which incorporates a temperature sensitivity is the so-called 'Brace–Goetze' model (see Molnar, 1989). In this model the lithosphere is assumed to deform by a combination of frictional sliding and power-law and Dorn-law creep mechanisms (see Table 1 for parameter ranges used in calculations). In this section we illustrate the rheological response of a 'Brace–Goetze' lithosphere to the burial of a radiogenic basement beneath a cover sequence, using the thermal models outlined in the preceding section (e.g. Figs 5 & 6). We assume a compositional stratification of the lithosphere such that the strength-limiting phase in the cover sequence is quartz, while in the basement it is feldspar and in the mantle it is olivine (the rheological parameters used for the various flow laws are listed in Table 1). Details of the mechanical modelling follow the outline given by Sandiford *et al.* (1991).

Before discussing the results of numerical calculations performed using the 'Brace–Goetze' model, it is worth summarising some of the limitations of this kind of modelling. Most importantly, the uncertainty in the
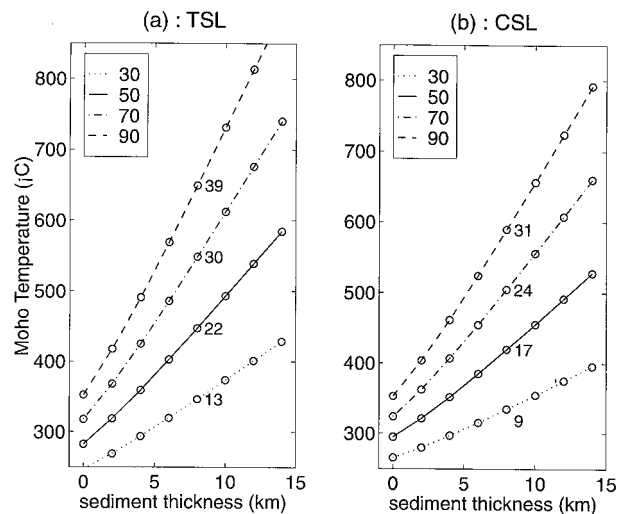

Fig. 6. Illustration showing the variation in Moho temperature resulting from the progressive burial of a radioactive basement. We assume that Moho depth is constant (40 km), independent of sedimentary cover thickness, as appropriate to an isostatically balanced crustal section in which variations in sediment thickness reflect variations in crustal stretching. Solutions are plotted for a range in q_c (= 30, 50, 70 and 90 mWm^{-2}) by modifying the value of H_i, other parameters are as for Fig. 5. (a) Solutions for the thermally stabilised lithosphere (TSL). (b) Solutions for the compositionally stabilised lithosphere (CSL). The number alongside each curve represents the average gradient expressed in units of °C/km^{-1}.

Table 1. Values of parameters used in calculations. Details of modelling procedure are outlined by Sandiford et al. (1991)

z_c	crustal thickness	40 km
z_l	lithospheric thickness	225 km
k	thermal conductivity	3 Wm^{-1} K^{-1}
μ	coefficient of friction	0.85
A_c	power-law creep, pre-exponential constant (cover)	5×10^{-6} s^{-1} MPa^{-3}
A_b	power-law creep, pre-exponential constant (basement)	5×10^{-2} s^{-1} MPa^{-3}
A_m	power-law creep, pre-exponential constant (mantle)	7×10^4 s^{-1} MPa^{-3}
Q_c	power-law creep, activation energy (cover)	1.9×10^5 J mol^{-1}
Q_b	power-law creep, activation energy (basement)	2.8×10^5 J mol^{-1}
Q_m	power-law creep, activation energy (mantle)	5.2×10^5 J mol^{-1}
σ_m	Dorn-law creep, threshold stress (mantle)	5.7×10^5 MPa
Q_d	Dorn-law creep, activation energy (mantle)	5.4×10^4 J mol^{-1}

material constants governing flow and fracture of rocks implies very large uncertainties in the strength of the lithosphere (see discussion by Molnar, 1989). Similarly, uncertainties in the thermal structure of lithosphere lead to large uncertainties in calculated strength. For example, an uncertainty in the Moho temperature of 100°C produces a factor of 2 error in calculated strength at a given strain rate or an order of magnitude error in strain rate at a given strength (e.g. Molnar, 1989). While absolute estimates of strength (or strain rate) are very uncertain, the variations in strength accompanying changes in other environmental variables, such as temperature, are likely to be far more robust. In the discussion below we concentrate on relative changes in strength accompanying changes in thermal regime during progressive burial of a 'hot' basement sequence. For the 'Brace–Goetze' lithosphere, the vertically-integrated creep strength of the lithosphere is usually defined for a specified strain rate. However, it is often geologically more reasonable to think of the strain rate that would apply to a 'Brace–Goetze' lithosphere at a given strength (F_l). This parameter F_l is perhaps best interpreted as the magnitude of the tectonic driving force.

Figure 7 shows the strain rate that applies for our model lithosphere for a range in applied tectonic forces (F_l) as the reference lithosphere is buried progressively beneath a sedimentary cover. This figure illustrates the sensitivity of the 'Brace–Goetze' lithosphere to thermal regimes, and particularly to the deep crustal thermal regimes. While the absolute magnitudes of the calculated strain rates are so uncertain as to be meaningless, the relative changes in strain rate accompanying burial are likely to be much more significant. The horizontal bars in Fig. 7 show that an increase in burial of 5 km can change the effective strain rate by 3–4 orders of magnitude at driving forces of 5×10^{12} N m^{-1}. While Fig. 7 shows that the depth of a radioactive layer can have a profound effect on the strength of the lithosphere, we should also expect that it is sensitive to the total amount of heat contributed by the 'hot' layer. Figure 8 illustrates the effect of varying the heat production in a enriched 'basement' buried beneath a 10-km-thick sedimentary blanket. Varying the total

amount of heat contributed by 20 mWm^{-2} produces a corresponding variation in strain rate of about 3 orders of magnitude at a specified strength. Figure 9 illustrates the relative effects of sediment thickness and crustal heat contributions on the strength (at a strain rate of 10^{-16} s^{-1}). For the parameter range appropriate to the northern Flinders Ranges (i.e. sedimentary thickness of $\sim$10 km and $q_c\sim$70 mWm^{-2}), a 5 km change in the thickness of the sedimentary pile produces a similar effect to a change in total basement heat production of about 20 mWm^{-2}.

Given that geologically significant strain rates at lithospheric scales range only over about 4 orders of
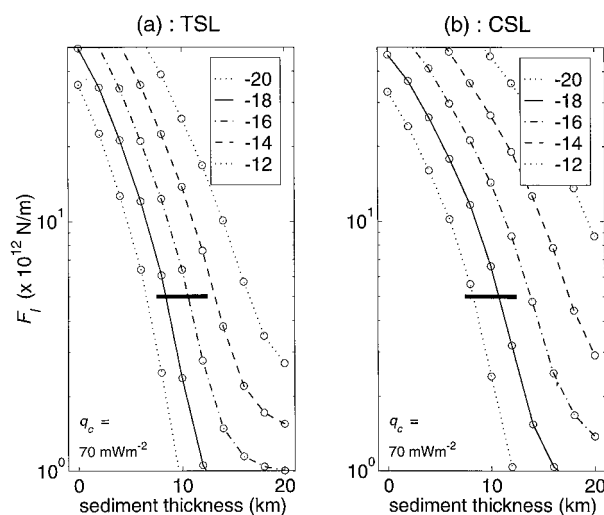

Fig. 7. Illustration of the rheological effects of progressive burial of a radioactive basement using a 'Brace–Goetze' rheological model as discussed in the text, and the thermal parameter range used in Fig. 5. We show the calculated lithospheric strength (F_l) for a range of effective strain rates ($=10^{-12}$, 10^{-14}, 10^{-16}, 10^{-18} and 10^{-20} s^{-1}). The strength parameter (F_l) can be best viewed as the magnitude of the tectonic force driving deformation. For constant values of F_l, an increase in the burial of the basement sequence by 5 km results in an increase in strain rate of up to four orders of magnitude for the thermally stabilised lithosphere (a) and three orders of magnitude for the compositionally stabilised lithosphere (b), as indicated by the solid bar at $F_l = 5 \times 10^{12}$ Nm^{-1}. Note that while the absolute values of the calculated strain rates at a given strength (or strengths at a given strain rate) are highly uncertain, rather more confidence is attached to estimates of the relative changes that accompany a given change in the thermal state (e.g. Molnar, 1989).
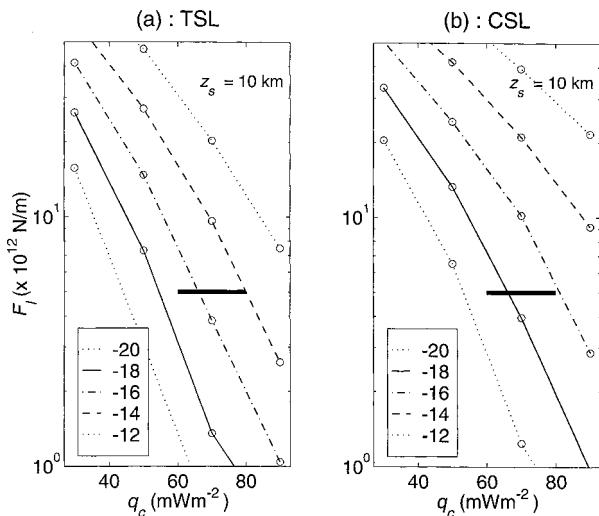
Fig. 8. Illustration of the dependence of lithospheric strength on total crustal heat production for a range of strain rates ($=10^{-12}$, 10^{-14}, 10^{-16}, 10^{-18} and 10^{-20} s^{-1}), with the heat production maxima (z_i) at a depth of 10 km.

magnitude (10^{-16} to 10^{-12} s^{-1}), the calculations summarised in Figs 7 and 8 point to the potentially profound (even extraordinary) role that a sedimentary blanket may play in localising deformation. Indeed, these calculations seem to provide a simple physical explanation for why significant Delamerian deformation is limited to regions where the basement is covered by a relatively thick sedimentary blanket. They also provide a plausible explanation for the intrabas-
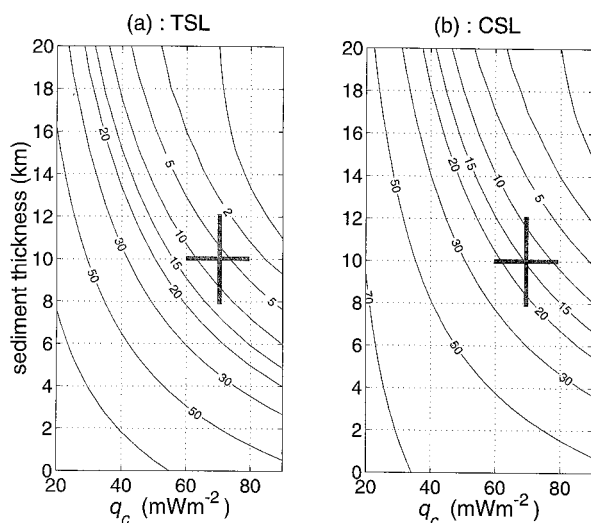

Fig. 9. Illustration of the relative effect of changes in sediment thickness and total crustal heat contributions on the strength of the lithosphere (at a strain rate of 10^{-16} s^{-1}). Note that while the contours are for absolute strength ($\times10^{12}$ N m^{-1}), the absolute values are extremely uncertain, and the diagram should only be used to illustrate relative effects. For example, the solid bars illustrate that for the parameter range appropriate to the northern Flinders Ranges (i.e. sedimentary thickness of ~10 km and q_c~70 mWm^{-2}), a 4 km change in the thickness of the sedimentary pile produces a similar effect to a change in total basement heat production of about 20 mWm^{-2}.

inal variations in strain observed between the northern and central Flinders Ranges, although we note that the available heat flow data from this region are not sufficiently dense (nor reliable) to preclude significant lateral variations in heat production in the basement rocks being responsible for the observed variation in deformation intensity.

CONCLUSIONS

The general correspondence between Delamerian deformation intensity and anomalous heat flow (averaging 90 mWm^{-2}) in the Flinders Ranges, suggests that thermal weakening of the crust has played a significant role in localising deformation in the northern and central, intracratonic parts of the Adelaide fold belt. However, the somewhat more intimate correspondence between the deformation intensity and thickness of the sedimentary sequence, both at the basin-wide and intrabasinal scale, suggests a pre-eminent role of sedimentary blanket thickness. The Neo-Proterozoic sedimentary thickness varies by up to 14 km across the Adelaide fold belt environment, with local intrabasinal variations of 4 km between the northern and central Flinders Ranges segments. The principal role of this variation in sedimentary blanket thickness is thermal and mediated by the depth to, and heat production in, an exceptionally 'hot' Meso-Proterozoic basement sequence. Our calculations show that for the thermal parameter range appropriate to the Flinders Ranges, Moho temperatures vary by between 25 and 35°C for every additional kilometre of sediment deposited on this basement complex (see also Cull and Conley, 1983), with 4 km of additional sediment enough to induce a 3 orders of magnitude change in the rheological response of a temperature sensitive 'Brace–Goetze' lithosphere to an imposed tectonic driving force.

Our analysis has important implications for the factors associated with localising intracratonic deformation and basin inversion. Firstly, if we are correct in our analysis that the spatial distribution of deformation in the Flinders Ranges is controlled by sedimentary blanket thickness then it demands that the lithosphere be very sensitive to the thermal state of the deeper crust, as is implicit in the 'Brace–Goetze' model. Secondly, the analysis may provide an important framework for understanding the general process of basin inversion. Basins may be expected to be inherently weak whenever a radiogenic basement is buried to significant depths, with the magnitude of the weakening effect dependent not only on the depth of the basin but also the amount of heat produced in the basement sequence.

REFERENCES

Brace, W. F. and Kohlstedt, D. L. (1980) Limits on lithospheric strength imposed by laboratory experiments. *Journal of Geophysical Research* **85**, 6248–6252.

Coney, P. J., Edwards, A., Hine, R., Morrison, F. and Windrim, D. (1990) The regional tectonics of the Tasman orogenic system, eastern Australia. *Journal of Structural Geology* **12**, 519–544.

Cull, J. P. (1982) An appraisal of Australian heat flow data. *BMR Journal of Australian Geology and Geophysics* **7**, 11–21.

Cull, J. P. and Conley, D. (1983) Geothermal gradients and heat flow in Australian sedimentary basins. *BMR, Journal of Australian Geology and Geophysics* **8**, 329–337.

England, P. C. (1987) Diffuse continental deformation: length scales, rates and metamorphic evolution. *Philosophical Transactions of the Royal Society* **A321**, 17,561–17,579.

Houseman, G. A., Cull, J. P., Muir, P. M. and Paterson, H. L. (1989) Geothermal signatures of uranium ore deposits on the Stuart Shelf of South Australia. *Geophysics* **54**, 158–170.

Jaupart, C. (1983) Horizontal heat transfer due to radioactivity contrasts: causes and consequences of the linear heat flow relation. *Geophysical Journal of the Royal Astronomical Society* **75**, 411–435.

Jenkins, R. J. F. (1990) The Adelaide Fold Belt: Tectonic reappraisal. In *The Evolution of a Late Precambrian–Early Palaeozoic Rift Complex: The Adelaide Geosyncline*, eds J. B. Jago and P. S. Moore, pp. 396–420. Geological Society of Australia Special Publication, **16**.

Jenkins, R. F. J. and Sandiford, M. (1992) Observations on the tectonic evolution of the southern Adelaide fold Belt. *Tectonophysics* **214**, 27–36.

Johnson, J. P. and Cross, K. C. (1995) U–Pb geochronological constraints on the genesis of the Olympic Dam Cu–U–Au–Ag deposit, South Australia. *Economic Geology* **90**, 1046–1063.

Lachenbruch, A. H. (1968) Preliminary geothermal model of the Sierra Nevada. *Journal of Geophysical Research* **73**, 6977–6989.

Marshak, S. and Flottmann, T. (1996) Structure and origin of the Fleurieu and Nackarra Arcs in the Adelaide Fold Belt, South Australia: salient and recess development in the Delamerian Orogeny. *Journal of Structural Geology* **18**, 891–908.

Mildren, S. and Sandiford, M. (1995) A heat refraction mechanism for low-*P* metamorphism in the northern Flinders Ranges, South Australia. *Australian Journal of Earth Sciences* **42**, 241–249.

Molnar, P. (1989) Brace–Goetze strength profiles, the partitioning of strike-slip and thrust faulting at zones of oblique convergence and the stress-heat flow paradox of the San Andreas Fault. In *Fault Mechanics and Transport Properties of Rocks*, eds B. Evans and T.-F. Wong, pp. 435–460. Academic Press, London.

Neil, E. A. and Houseman, G. (1997) Geodynamics of the Tarim Basin and the Tian Shan in central Asia. *Tectonics* **16**, 571–584.

Ord, A. and Hobbs, B. (1989) The strength of the continental crust. *Tectonophysics* **158**, 269–289.

Paul, E., Flottman, T. and Sandiford, M. (1999) Structural geometry of the Northern Flinders Ranges in the Adelaide Fold Belt, South Australia. *Australian Journal of Earth Sciences* (in press).

Preiss, W. (1987) The Adelaide geosyncline, late Proterozoic stratigraphy sedimentation and tectonics. *Geological Survey of South Australia, Bulletin* **53**, 1–438.

Rogers, J. (1995) Lines of basement uplift within the external parts of orogenic belts. *American Journal of Science* **42**, 233–240.

Sandiford, M., Martin, N., Zhou, S. and Fraser, G. (1991) Mechanical consequences of granite emplacement during high-*T*, low-*P* metamorphism and the origin of 'anticlockwise' *PT* paths. *Earth and Planetary Science Letters* **107**, 164–172.

Sandiford, M., Hand, M. and McLaren, S. (1998) High geothermal gradient metamorphism during thermal subsidence. *Earth and Planetary Science Letters* **163**, 149–165.

Sass, J. H. and Lachenbruch, A. H. (1975) Thermal regime of the Australian Continental Crust. In *The Earth: its Origin, Evolution and Structure*, ed. M. W. McElhinny, p. 301. Academic Press.

Sonder, L. and England, P. (1986) Vertical averages of rheology of the continental lithosphere; relation to thin sheet parameters. *Earth and Planetary Science Letters* **77**, 81–90.

Zhou, S. and Sandiford, M. (1992) On the stability of isostatically compensated mountain belts. *Journal of Geophysical Research* **97**, 14,207–14,221.

Zielhuis, A. and van der Hilst, R. D. (1996) Upper-mantle shear velocity beneath eastern Australia from inversion of waveforms from Skippy portable arrays. *Geophysical Journal International* **127**, 1–16.